

An Experimental and Theoretical Analysis of Foam Formation in the Sour Gas Sweetening Process

Mahmod Fatemi¹ and Bahram Hashemi Shahraki^{2,*}

¹ Ph.D. Candidate, Department of Chemical Engineering, Petroleum University of Technology, Ahwaz, Iran

² Associate Professor, Department of Gas Engineering, Petroleum University of Technology, Ahwaz, Iran

Received: December 18, 2017; *revised:* January 03, 2018; *accepted:* January 28, 2018

Abstract

Use of amine solutions for the removal of acid gases such as carbon dioxide (CO₂) and hydrogen sulfide (H₂S) from natural gas is the most common method, and, in this process, operational problems because of foaming are reported. Foaming can lead to the entrainment of liquid into downstream process equipment and might result in a situation in which the process specifications cannot be met for acid gases. Alkanolamines in general have a negative effect on downstream process equipment, and the loss of amines has a negative effect on the health, safety, and environment (HSE). The foam reducing agents are often used to reduce the risk of heavy foaming in amine plants. This study concerns with foaming in amine-based CO₂ plants. To investigate foaming related to CO₂ removal from natural gas by amine solutions, the fundamental theory of foaming in gas-liquid contactors was first reviewed. Then, experimental techniques related to this phenomenon in diethanolamine (DEA)/CO₂ absorbers were considered. After that, foaming of diethanolamine solution polluted with different impurities was noticed, and the tendency of foam was measured by considering their foaming indices. To analyze the experimental measurements and experimental observations, a mathematical model was developed too. The model could justify the experimental measurement reasonably.

Keywords: Sour Gas, Foam Stability, Foaming Ability, DEA Solution, Liquid Hydrocarbon

1. Introduction

Sweetening of sour gas by aqueous solutions of alkanolamine is performed in absorber towers. Mass transfer is being conducted between solution and the sour gas in this vessel. The vessel contains some trays which are designed to produce froth by violently bubbling gas through the treating solution. The bubble walls in the froth act as mass transfer area for the removal of the gas borne contaminants. The froth bubbles break quickly enough for the treating liquid to pass down to the next tray in the column before the gas flow is restricted. If the gas/liquid disengagement time is increased, the froth will remain in the vapor space of the tray, and the gas flow will be restricted. This hydraulic restriction is detected as a differential pressure above and below the froth in the vapor space. This condition is described as solution foaming. A variety of solution contaminants and operating conditions can cause

* Corresponding Author:

Email: hashemi_ba@put.ac.ir

froth to stabilize into foam. The survey of the previous works shows that the foaming phenomenon has usually been studied qualitatively rather than quantitatively because of the complexity (WL, 1973; Smith, 1979). Gilyazetdinov and Matishev (1990) reported that the pure amine solutions do not form stable foams, but this phenomenon is observed once some other components are presented in the treating solution. Stewart and Lanning (1994) presented that the generation of a certain amount of foam or froth on each tray of the absorber tower is normal in alkanolamine treating process, but this foam is not stable and quickly breaks down into solution. McCarthy and Trebble (1996) reported that the addition of contaminants to a system, which already has the tendency to foam, did increase foaming significantly. Cummings et al. (2003) studied contaminants and their effects on gas sweetening system operations and found out that the dissolved liquid hydrocarbons may cause amine solutions to foam. An experimental work on investigating the foam stability and the foaming ability of dilute aqueous solution of the diglycerol fatty acid esters has been conducted (Shrestha et al., 2007). The stability of foam formation in the presence of the floating contaminants such as n-pentanol and n-octanol has been examined (Wang and Yoon, 2008). de Villiers et al. (2009) found out that the closed nature of the amine circulation loop could lead to a build-up of solids, salts, amine breakdown products, and other surface-active species, which results in an increased foaming tendency. Chen et al. (2011) reported that the liquid hydrocarbon and organic acid increase the foaming tendency and the foam stability of amine solutions by various extents. Bournival et al. (2014) discovered that the addition of hydrophobized submicron particles increased the gas holdup, in most cases; increasing the concentration of particles decreases the stability of the froth phase with the tested surfactants. Khazaei et al. (2014) studied the surface tension of the multi-component mixtures at different temperatures and presented a model based on the neural network analyses. The lifetime of moderately stable foams depends largely on surfactant concentration below the critical micelle concentration (CMC), but this effect does not scale linearly with surfactant concentration (Lioumbas et al., 2015). A model used to study the sensitivity of foaming tendency related to designing and operating parameters in CO₂ absorption processes has also been presented (Thitakamol et al., 2015). Added corrosion inhibitor into the solution of aqueous methyl diethanolamine (MDEA) increased the foam breaking time and the foam volume (Alhseinat et al., 2015). Ranjbar et al. (2015) investigated the effect of some nanoparticles such as γ -Al₂O₃ and MgO on the surface tension of the nanofluid of tri ethylene glycol (TEG). They found out that the surface tension initially decreases with increasing particle concentration, and the trend is then reversed; thus surface tension rises. Tavan et al. (2016) presented some notes on the process intensification of amine-based gas sweetening processes for better temperature distribution in contactor to reduce the amount of amine as a result of corrosion and foaming. They discovered that using mixed amine increases the foaming phenomena along the absorber. Rafati et al. (2016) found out that the solid particles such as iron oxide and calcium sulfate destabilize the foam due to the rapid destruction of bubbles in the presence of high density particles. Ke et al. (2016) studied foaming of formulated solvent UDS and improving foaming control in acid sweetening process of natural gas. According to their results, an increase in CO₂ loading enhanced foaming tendency. The effect of surfactants on the oil/brine interfacial tension was experimentally investigated by Mohammad Saki and Ali Reza Khaz'ali (2017) too.

According to the literature survey, few quantitative measurements of the onset of foaming with foaming agents are observed in the works of previous investigators. Also, there is not enough information about the stability of foam bubbles versus contaminant concentration. Moreover, foam collapse behavior with time is not seen in any previous research. In this work, the stability of formed foam of DEA solution in the presence of some impurities is analyzed and modeled. The foaming ability and foam stability of the solution are expressed quantitatively. The model predictions were consistent with experimental results. The nobility of the current work is that it seems that wet and

small bubbles collapse faster than dry and big polyhedral ones. Furthermore, the foaming tendency and the foam stability are found to improve with increasing some impurities concentration, while it was not the case with the others. In the presence of some impurities, foaming first increased with concentration but it decreased afterwards.

2. Materials and methods

2.1. Materials

Aqueous DEA (30 wt.% DEA and 70 wt.% de-aerated water) was used as the treated solution, and carbon dioxide was selected as the process gas. There are two categories of contaminants which cause the foam formation in amine systems: the contaminants added to the solution and those created within the process. Added contaminants include liquid hydrocarbons (resulted from the condensation of gaseous hydrocarbons), well treating fluids, antifoam agents, corrosion inhibitors, particulates, and lubricants in the form of aerosols. Contaminants created when treating the solution include basic and acidic amine degradation products, iron sulfide, and iron oxides (hydroxides). According to the previous investigation, liquid hydrocarbons and fine particles are important foaming agents in some plants (Abdi et al., 2001; Pauley et al., 1989). Therefore, gas oil, liquid n-hexane, and solid impurities were used as pollutant materials in this work. The chemical specifications and the sources of materials are summarized in Table 1. It should be noted that the real solid impurities were collected from one of the plants in the south of Iran. The component analysis of the solid impurities is listed in Table 2.

Table 1
Specifications and sources of chemicals used in the current work.

Chemical name	Molecular formula	CAS number	Molar mass	Purity	Source
DEA (diethanolamine)	C ₄ H ₁₁ NO ₂	[111-42-2]	105.14g·mol ⁻¹	99%	Aldrich
Carbone dioxide	CO ₂	[124-38-9]	44.01g·mol ⁻¹	98%	Roham Gas Company
Gas oil	C ₁₀ H ₂₀ to C ₁₅ H ₂₈	[68814-87-9]	-	97%	Abadan refinery
N-hexane	C ₆ H ₁₄	[110-54-3]	86.18g·mol ⁻¹	95%	Merck

Table 2
Components analysis of the solid impurities.

Component	Mole percent (%)
Fe ⁺³	40
Fe ⁺²	30
Heavy hydrocarbons	30

2.2. Method

The Bikerman's method was selected for conducting all the experiments. Figure 1 shows the schematic of the foaming set-up used for conducting the experiments. Each of the chemicals presented in Tables 1 and 2 was added to 1500 cc of the treated solution in every experiment, and pure CO₂ was

then allowed to flow into the impure solution. As soon as the process gas at a known volume flow rate of (G) is sparged into the liquid column, foam forms, and the height of foam rises as a function of time. The foam generation is accompanied by the bursting of bubbles too, which mainly occurs at the top of the foam, i.e. at the foam–air interface. This process continues until a condition is reached in which foam bubble generation and foam bubble contraction become equal. In this situation, the foam height remains constant which indicates that an equilibrium condition is established. Each experiment was repeated three times, and the results were recorded. The rate of foam collapse was very similar, and the error was less than 2%. The ratio of the volume of the produced foam to the volume flow rate of gas was calculated in each experiment. This index represented the foaming intensity (foaming index) of the solution. At equilibrium, once the foam height was stable, it was measured and recorded as $h = H_0$. Then, the gas flow to the test vessel was stopped and the shrinkage of foam height $h(t)$ versus time (t) was recorded. The experimental data are tabulated in Table 3. It was observed that while the foam height was dropping with time, the bubble size and shape were continuously changing in the foam. The size of bubbles in the foam was changing because the liquid from the bubble walls was draining, and with thinning of the walls, the small bubbles penetrated into the larger ones. The experiments revealed that the rate of foam height shrinkage ($-\frac{dh(t)}{dt}$) was proportional to $h(t)$ for all the systems. To analyze this observation, a mathematical model was developed.

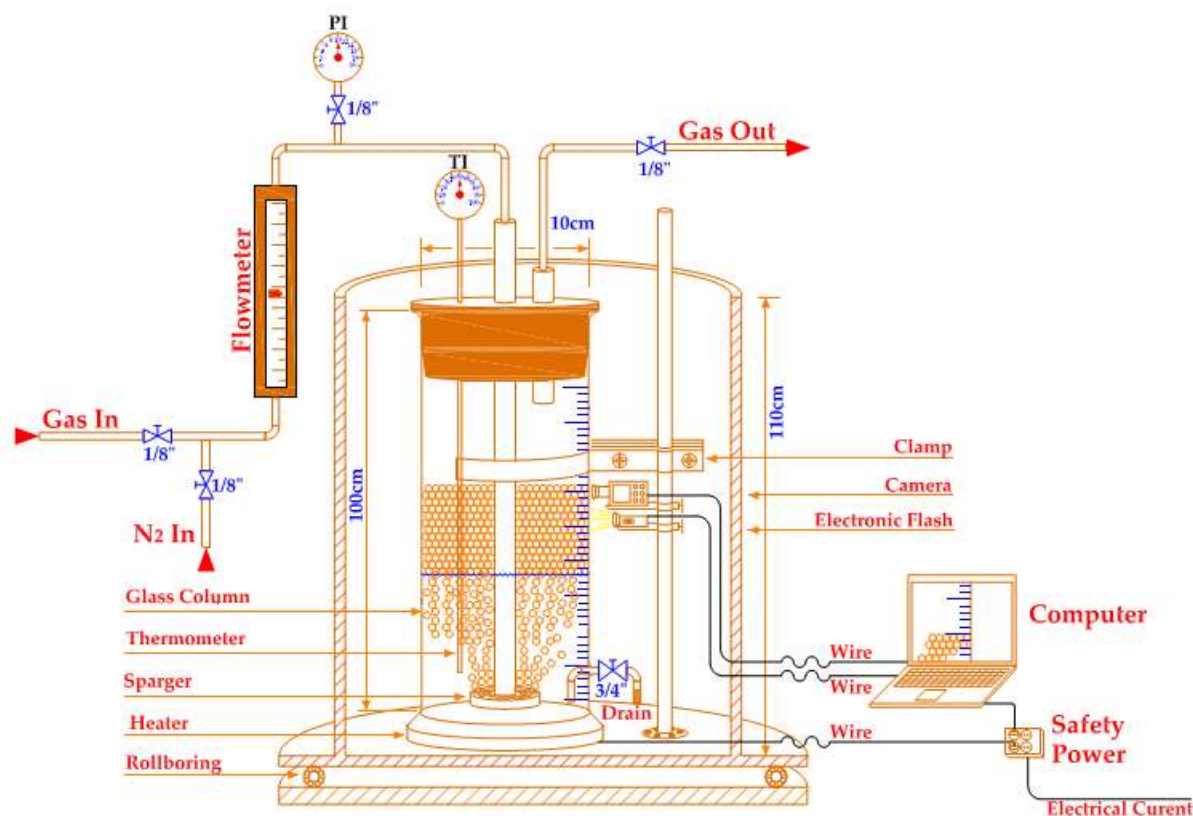


Figure 1

A schematic diagram of the foaming experimental setup.

Table 3

Experimental data.

Type of impurity	Time (s)	Impurities concentration			
		1400 ppm	1800 ppm	2200 ppm	2600 ppm

		h(cm)	h/H₀	h(cm)	h/H₀	h(cm)	h/H₀	h(cm)	h/H₀
Gas oil	0	39(H ₀)	1.00	44(H ₀)	1.00	44(H ₀)	1.00	42(H ₀)	1.00
	10	26	0.67	29	0.66	31	0.70	29	0.69
	15	24	0.62	26	0.59	25	0.57	23	0.55
	20	21	0.54	22	0.50	22	0.50	20	0.48
	30	17	0.44	17	0.39	17	0.39	16	0.38
	40	15	0.38	13	0.30	14	0.32	12	0.29
	50	13	0.33	12	0.27	11	0.25	10	0.24
	60	11	0.28	9	0.20	9	0.20	8	0.19
Σ(s)		27.53		31.06		31.06		29.67	
N-hexane	0	44(H ₀)	1.00	46(H ₀)	1.00	48(H ₀)	1.00	48(H ₀)	1.00
	10	33	0.75	36	0.78	38	0.79	39	0.82
	15	29	0.66	32	0.70	33	0.69	38	0.79
	20	26	0.59	28	0.61	30	0.63	35	0.72
	30	24	0.55	27	0.59	29	0.60	33	0.69
	40	23	0.52	25	0.54	27	0.56	32	0.67
	50	22	0.50	24	0.52	26	0.54	31	0.65
	60	21	0.48	23	0.50	25	0.52	29	0.60
Σ(s)		31.08		32.50		33.91		33.91	
Solid impurities	0	27(H ₀)	1.00	31(H ₀)	1.00	33(H ₀)	1.00	30(H ₀)	1.00
	10	16	0.59	18	0.58	19	0.58	18	0.60
	15	13	0.48	16	0.52	16	0.48	14	0.47
	20	11	0.41	13	0.42	13	0.39	11	0.35
	30	8	0.30	10	0.32	9	0.27	8	0.27
	40	6	0.22	7	0.23	7	0.21	6	0.19
	50	5	0.19	6	0.19	5	0.17	4	0.13
	60	4	0.15	5	0.16	4	0.12	3	0.10
Σ(s)		19.07		21.90		22.45		19.73	

3. Model development

To simplify the modeling of the complex process of foam shrinking, the bubbles in the foam were assumed to be all spherical having the same size. If \dot{r} is considered to be the rate of disappearance of one bubble in the foam, then the rate of bubble rupture in the whole column of foam is defined by:

$$-\frac{dN_{(t)}}{dt} = N_{(t)} \cdot \dot{r} \tag{1}$$

where, $N_{(t)}$ is the number of bubbles in foam at time t . The integration of Equation 1 leads to:

$$N_{(t)} = N_{(0)} \exp(-\dot{r} t) \tag{2}$$

where, $N_{(0)}$ is the number of bubbles in foam at $t=0$. Meanwhile, the liquid holdup in foam bubbles is $\varepsilon_{(t)}$, and that of gas in foam is $(1 - \varepsilon_{(t)})$; then, the amount of gas in foam at a height of $h_{(t)}$ is given by:

$$Q_G = A \cdot h_{(t)} (1 - \varepsilon_{(t)}) \quad (3)$$

where, A is the cross sectional area of the test vessel, and $h_{(t)}$ represents the height of foam at time t in the column. Now, if we assume that the volume of each bubble in the foam is $\bar{V}_{(t)}$ and the average radius of bubbles is $\bar{r}_{(t)}$, then we can write:

$$Q_G = N_{(t)} \bar{V}_{(t)} = N_{(t)} \left(\frac{4\pi \bar{r}_{(t)}^3}{3} \right) \quad (4)$$

Combining Equations 3 and 4 results in:

$$N_{(t)} \bar{V}_{(t)} = N_{(t)} \left(\frac{4\pi \bar{r}_{(t)}^3}{3} \right) = A \cdot h_{(t)} (1 - \varepsilon_{(t)}) \quad (5)$$

Equation 5 can be used at $t=0$ as follows:

$$N_{(0)} \cdot \bar{V}_{(0)} = A \cdot h_{(0)} (1 - \varepsilon_{(0)}) \quad (6)$$

Dividing Equation 5 by Equation 6 gives:

$$\frac{N_{(t)}}{N_{(0)}} = \frac{h_{(t)} (1 - \varepsilon_{(t)})}{h_{(0)} (1 - \varepsilon_{(0)})} \quad (7)$$

In the model, we assumed that the size of foam bubbles was independent of time although this was not the case in reality. This assumption permitted us to write $\varepsilon_{(t)} = \varepsilon_{(0)}$. As a result, Equation 7 is reduced to:

$$\frac{h_{(t)}}{h_{(0)}} = \frac{N_{(t)}}{N_{(0)}} = \exp(-\dot{r} t) \Rightarrow \ln \left(\frac{h}{H_0} \right) = -\dot{r} t \quad (8)$$

The parameters $H_0 = h_{(0)}$ at $t = 0$ and $h_{(t)} = h$ at time t were measured during the experiments. Equation 8 indicates that the graph of $\ln(\frac{h}{H_0})$ versus time is a straight line with a slope of $-\dot{r}$. If this relation is confirmed by the experimental measurement, then the developed model could be satisfactory. By calculating \dot{r} for different experiments, the speed of foam shrinkage is obtained, and the foam stability could be stated quantitatively. Once \dot{r} was found, the impurity that produces the most stable foam is recognized too. We proposed the model of bubbles generation and destruction based on their similarity to population growth and its decay.

4. Results and discussion

Table 3 represents the foam heights at different times during their shrinking process in DEA solution polluted with each of the contaminants such as gas oil, n-hexane, and solid impurities. Based on the experimental investigations done by McCarthy and Trebble (1996), liquid hydrocarbons, corrosion inhibitors, suspended solids, degradation products, and carboxylic acids produce foam in aqueous amine solutions. Chen et al. (2011) reported that liquid hydrocarbons and fine particles composed of ferrous

oxides or ferrous hydroxide in amine solutions might contribute to an increase in foaming tendency, which confirmed the effect of selected impurities on the foaming tendency of polluted amine solutions.

As shown in Table 3, the foaming indices of DEA/gas oil system are respectively 27.53 s, 31.06 s, 31.06 s, and 29.67 s at 1400 ppm, 1800 ppm, 2200 ppm, and 2600 ppm of gas oil concentration. In addition, this parameter is 19.07 s, 21.90 s, 22.45 s, and 19.73 s for DEA/solid impurities system at similar concentrations correspondingly. These data describe the sensitivity of foaming tendency of the system which slightly increased with impurity concentration first but then dropped. The behavior of the foam growth and collapse versus agent concentration has been analyzed by Chen et al. (2011), which justifies our results. They reported that foaming index increased slightly with Fe^{3+} concentration first, but peaked at a concentration of 0.2 mM; it then dropped and leveled off at higher concentrations. Hence, previous investigations justify our experimental results.

The plots of foam height versus time on a log-linear scale are shown in Figures 2, 3, 4, and 5 respectively. Each figure represents $\ln\left(\frac{h}{H_0}\right)$ versus time for different impurities in the solution but at the same concentration, while different figures are drawn for different concentrations of the pollutants. As it is seen in all the figures, the plot of $\ln\left(\frac{h}{H_0}\right)$ versus time on a log-linear scale is a straight line, which confirms the proposed model. However, the slope of the line does change or the line breaks after some intervals of time; in other words, the rate of breakage of foam bubbles decreases after a period of time. This might be due to the change of the shape and size of the foam bubbles with time, which contradicts the assumptions of $\bar{V}(t) = \bar{V}(0)$ in the model. Actually, the foam bubbles are spherical first, but they change to polyhedral later. At the beginning of foam decay, the foam bubbles are wet, small, and spherical, but as time proceeds, they become dry, big, and polyhedral. The experiments state that the wet and small bubbles are decayed at a faster rate than the dry and big polyhedral ones. This might be due to the fact that the pressure of gas inside the small spherical bubbles is higher than that of gas in polyhedral ones.

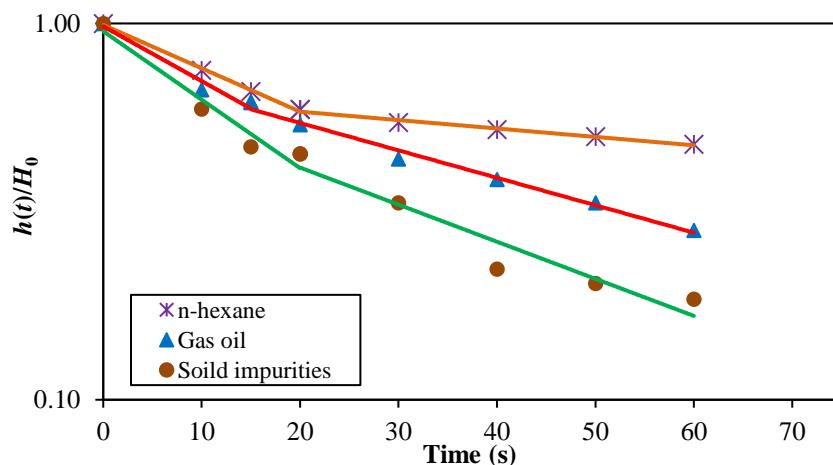


Figure 2

Variations of $\left(\frac{h(t)}{H_0}\right)$ versus time for the aqueous solution of DEA in the presence of 1400 ppm of different impurities.

According to Figure 2, the slopes of the shrinkage of the foam height for n-hexane, gas oil, and solid impurities are $(-0.027, -0.005)$, $(-0.034, -0.017)$, and $(-0.042, -0.022)$ respectively at 1400 wt. ppm of the pollutant concentrations. Moreover, at a pollutant concentration of 1800 ppm, these parameters are

(-0.025, -0.005), (-0.034, -0.021), and (-0.045, -0.026) respectively according to Figure 3. This trend in slope change is also visible in Figures 4 and 5, which are plotted for pollutant concentrations of 2200 wt. ppm and 2600 wt. ppm. The experimental measurements revealed that n-hexane produced more foam at the highest foam stability than the other impurities.

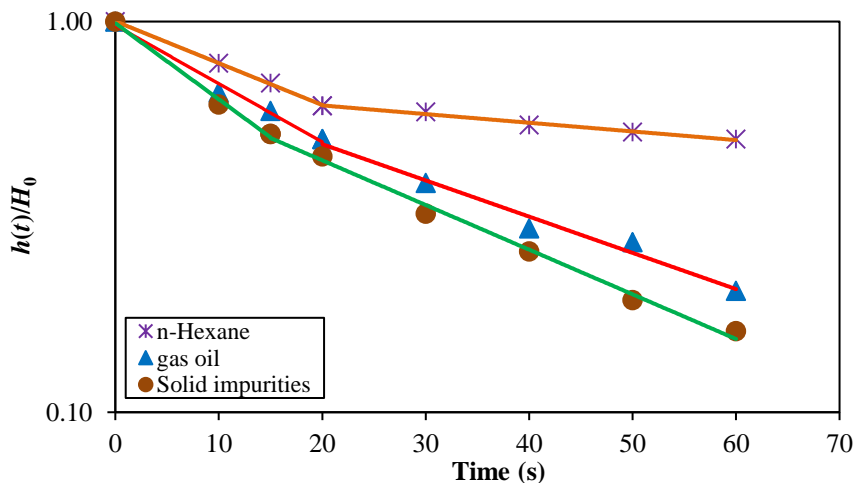


Figure 3

Variations of $\left(\frac{h(t)}{H_0}\right)$ versus time for the aqueous solution of DEA in the presence of 1800 ppm of different impurities.

The foaming tendency and the foam stability of DEA solution were found to rise with increasing n-hexane concentration. However, in cases of gas oil and solid impurities, foaming of the solution first increased but it then dropped with the impurity concentration. The empirical observations and calculated amount of foam indices revealed this sort of behavior of DE /gas oil and DEA/solid impurity systems. This might be due to the saturation of the amine with the impurity molecules and the multiplicity behavior of the solution.

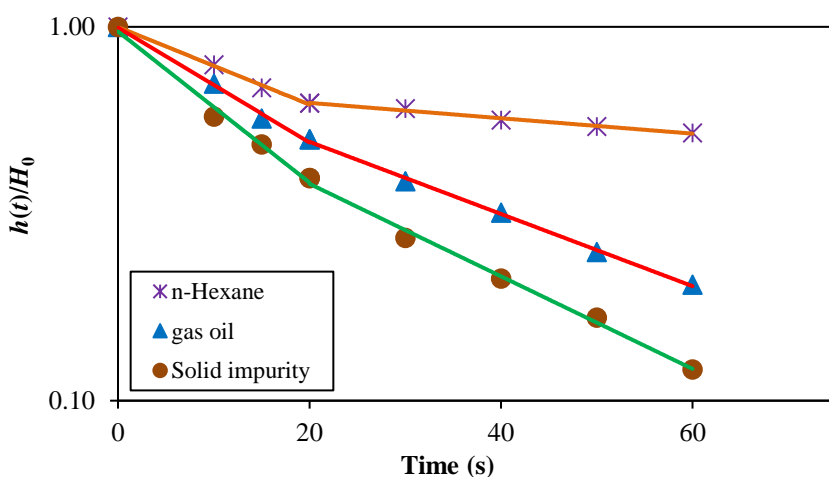


Figure 4

Variations of $\left(\frac{h(t)}{H_0}\right)$ versus time for the aqueous solution of DEA in the presence of 2200 ppm of different impurities.

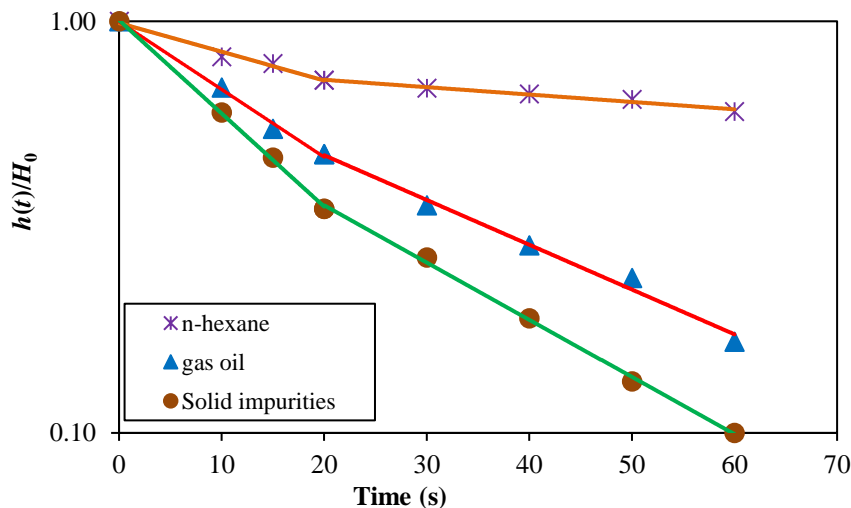


Figure 5

Variations of $\left(\frac{h(t)}{H_0}\right)$ versus time for the aqueous solution of DEA in the presence of 2600 ppm of different impurities.

5. Conclusions

In this study, the effect of various contaminants on the foaming of the aqueous DEA solution was evaluated. The foaming ability of the polluted solution and the stability of the produced foam were measured at different pollutant concentrations. The experimental work revealed that:

- Chain hydrocarbons such as liquid n-hexane enhance the foam stability and foaming tendency of DEA solution. However, gas oil indicated weaker foam stability than n-hexane. It is stated that the existence of hydrocarbons heavier than n-hexane in gas oil might play the de-foaming function in the solution (Wasan et al., 1994).
- In all the experiments, the speed of foam decay was fast first, then, it slowed down after a period of time. This observation revealed that small and spherical bubbles in wet foams burst sooner than large polyhedral bubbles in dry foams.
- An increase in the concentration of n-hexane in DEA solution enhanced foaming intensity of the solution and the stability of the produced foam, whereas, for other impurities examined in this work, foaming ability passed through a maximum at some concentration of pollutants and then decreased at higher pollutant concentrations.
- The results obtained for the effect of impurities were encouraging, but further studies are clearly required to check the effect of mixed pollutants on enhancing foaming.

The proposed model can be used in the gas sweetening systems by amine solutions. According to this model, liquid hydrocarbons and solid particles enhance the foaming tendency and foam stability, so, in order to prevent foam formation, the concentration of these materials should be reduced below the critical micelle concentration in the amine solution. Therefore, the suitable filtration and removal of solid particulate from circulating amine solution inhibits foaming in contactors. Finally, the pre-separation of gas contaminants by mechanical separators before entering the contactor can vastly inhibit foaming.

Nomenclature

A	: Foam column cross section area (m ²)
G	: Gas injection flow rate (Nm ³ /hr.)
H_0	: Initial foam height (cm)
$h(0)$: Foam height at $t=0$ (cm)
$h(t)$: Foam height in time (cm)
$N(0)$: Number of bubbles in foam at $t=0$
$N(t)$: Number of bubbles in foam at time t
Q_G	: Total gas flow in foam column (m ³)
\bar{r}	: Bubble average radius (mm)
\dot{r}	: Average rate of bubble disappearance in time (s ⁻¹)
t	: Time (s)
\bar{V}	: Average bubble volume (m ³)
Σ	: Foaminess index (s)
ε	: The accumulation of liquid in the foam column

References

- Abdi, M.A., Golkar, M., and Meisen, A., Improve Contaminant Control in Amine Systems, *Hydrocarbon Processing*, Vol. 80, No. 10, p. 102, 2001.
- Alhseinat, E., Amr, M., Jumah, R., and Banat, F., Removal of MDEA Foam Creators Using Foam Fractionation: Parametric Study Coupled with Foam Characterization, *Journal of Natural Gas Science and Engineering*, Vol. 26, p. 502-509, 2015.
- Bournival, G., Du, Z., Ata, S., and Jameson, G., Foaming and Gas Dispersion Properties of Non-ionic Frothers in the Presence of Hydrophobized Submicron Particles, *International Journal of Mineral Processing*, Vol. 133, p. 123-131, 2014.
- Chen, X., Freeman, S.A., and Rochelle, G.T., Foaming of Aqueous Piperazine and Monoethanolamine for CO₂ Capture, *International Journal of Greenhouse Gas Control*, Vol.5, No. 2, p. 381-386, 2011.
- Cummings, A.L., Street, D., and Lawson, G., Contaminants and Their Effects on Operations—Yes! You Can Have Better Operating Amine and Glycol Systems!, *The Brimstone Sulfur Conference*, Banff, Alberta, (May), 2003.
- De Villiers, W., Green, W., Shivelor, G., and Chemtech, S., DEA Treater Revamp Targets Foaming, *the 2009 Spring National Meeting*, 2009.
- Gilyazetdinov, L. and Matishev, V., Prevention of Foaming in Amine Treatment of Natural Gas, *Chemistry and Technology of Fuels and Oils*, Vol. 26, No. 5, p. 250-258, 1990.
- Ke, Y., Shen, B., Sun, H., Liu, J., and Xu, X., Study on Foaming of Formulated Solvent UDS and Improving Foaming Control in Acid Natural Gas Sweetening Process, *Journal of Natural Gas Science and Engineering*, Vol. 28, p. 271-279, 2016.
- Khazaei, A., Parhizgar, H., and Dehghani, M.R., The Prediction of Surface Tension of Ternary Mixtures at Different Temperatures Using Artificial Neural Networks, *Iranian Journal of Oil & Gas Science and Technology*, Vol. 3, No. 3, p. 47-61, 2014.

- Lioumbas, J.S., Georgiou, E., Kostoglou, M., and Karapantsios, T.D., Foam Free Drainage and Bubbles Size for Surfactant Concentrations below the CMC, *Colloids and Surfaces A: Physicochemical and Engineering Aspects*, Vol. 487, p. 92-103, 2015.
- McCarthy, J. and Trebble, M., An Experimental Investigation into the Foaming Tendency of Diethanolamine Gas Sweetening Solutions, *Chemical Engineering Communications*, Vol. 144, No. 1, p. 159-171, 1996.
- Pauley, C., Hashemi, R., and Caothien, S., Ways to Control Amine Unit Foaming Offered, *Oil and Gas Journal (USA)*, Vol. 87, No. 50, p. 67, 1989.
- Rafati, R., Haddad, A.S., and Hamidi, H., Experimental Study on Stability and Rheological Properties of Aqueous Foam in the Presence of Reservoir Natural Solid Particles, *Colloids and Surfaces A: Physicochemical and Engineering Aspects*, Vol. 509, p. 19-31, 2016.
- Ranjbar, H., Khosravi-Nikou, M.R., Safiri, A., Bovard, S., and Khazaei, A., Experimental and Theoretical Investigation on the Nanofluid Surface Tension, *Journal of Natural Gas Science and Engineering*, Vol. 27, No. 3, p. 1806-1813, 2015.
- Saki, M. and Khaz'ali, A.R., Influence of Surfactant Type, Surfactant Concentration and Salinity on Interfacial Tension of a Brine/Live Oil/Surfactant Fluid System: a Case Study of Iranian Asmari Oil Reservoir, *Iranian Journal of Oil & Gas Science and Technology*, Vol. 6, No. 1, p. 01-12, 2017.
- Shrestha, L.K., Saito, E., Shrestha, R.G., Kato, H., Takase, Y., and Aramaki, K., Foam Stabilized by Dispersed Surfactant Solid and Lamellar Liquid Crystal in Aqueous Systems of Diglycerol Fatty Acid Esters, *Colloids and Surfaces A: Physicochemical and Engineering Aspects*, Vol. 293, No. 1, p. 262-271, 2007.
- Smith, R. F., Curing Foam Problems in Gas Processing, *Oil & Gas Journal*, Vol. 77, No. 31, p. 186, 1979
- Stewart, E.J. and Lanning, R.A., Reduce Amine Plant Solvent Losses; Part 1, Hydrocarbon Processing; (United States), Vol. 73, No. 5, 1994.
- Tavan, Y., Gholami, H., and Shahhosseini, S., Some Notes on Process Intensification of Amine Based Gas Sweetening Process for Better Temperature Distribution in Contactor to Reduce the Amount of Amine as a Result of Corrosion and Foaming, *Journal of Loss Prevention in the Process Industries*, Vol. 41, No. 169-177, 2016.
- Thitakamol, B., Veawab, A., and Aroonwilas, A., Development of a Mechanistic Foam Model for Alkanolamine-based CO₂ Absorbers Fitted With Sheet-metal Structured Packing, *International Journal of Greenhouse Gas Control*, Vol. 33, p. 77-88, 2015.
- Wang, L. and Yoon, R.-H., Effects of Surface Forces and Film Elasticity on Foam Stability, *International Journal of Mineral Processing*, Vol. 85, No. 4, p. 101-110, 2008.
- Wasan, D., Koczo, K., and Nikolov, A., Mechanisms of Aqueous Foam Stability and Antifoaming Action with and without Oil: a Thin-film Approach, ACS Publications, 1994.
- WL, S., Filter DEA Treating Solution, *Hydrocarbon Processing*, Vol. 52, No. 8, p. 95-96, 1973.